Research Article

Visible-Light-Driven Catalytic Dehalogenation of Trichloroacetic Acid and α-Halocarbonyl Compounds: Multiple Roles of Copper

Abigail J. Thillman, Erin C. Kill, Alexander N. Erickson, and Dian Wang*

Cite This: ACS Catal. 2025, 15, 3873−3881

Read Online

ACCESS | 📊 Metrics & More | 📖 Article Recommendations | 🆂🅸 Supporting Information

ABSTRACT: Herein, we report the reaction development and mechanistic studies of visible-light-driven Cu-catalyzed dechlorination of trichloroacetic acid for the highly selective formation of monochloroacetic acid. Visible-light-driven transition metal catalysis via an inner-sphere pathway features the dual roles of transition metal species in photoexcitation and substrate activation steps, and a detailed mechanistic understanding of their roles is crucial for the further development of light-driven catalysis. This catalytic method, which features environmentally desired ascorbic acid as the hydrogen atom source and water/ethanol as the solvent, can be further applied to the dehalogenation of a variety of halocarboxylic acids and amides. Spectroscopic, X-ray crystallographic, and kinetic studies have revealed the detailed mechanism of the roles of copper

in photoexcitation, thermal activation of the first C−Cl bond, and excited-state activation of the second C−Cl bond via excited-state chlorine atom transfer.

KEYWORDS: dechlorination, photocatalytic mechanisms, inner-sphere photochemistry, excited-state chlorine transfer, copper catalysis
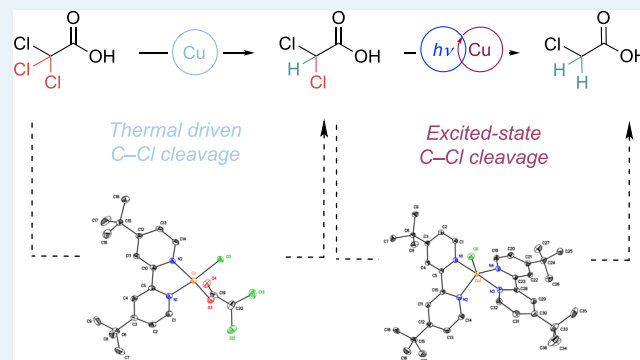
INTRODUCTION

For the last two decades, the field of organic chemistry has enjoyed remarkable advances in new synthetic methods developed through visible-light-driven catalysis (e.g., photoredox catalysis, metallaphotoredox catalysis).[1] The success of this reaction class can be largely attributed to the efficient harnessing of visible light energy for the activation of organic substrates, which facilitates the generation of highly reactive radical intermediates. This visible-light-driven activation leads to unprecedented reactivity and selectivity, contrary to thermal-driven reactions. Therefore, the exploration of new reaction pathways to leverage visible light will likely lead to the further development of new and improved catalytic processes.

The overwhelming majority of recent examples in visible-light-driven catalysis operate through an outer-sphere mechanism, where the substrate undergoes activation via single electron transfer or energy transfer with the photoexcited species. In contrast, an inner-sphere mechanism, where the excited-state species participates in bond-forming or bond-breaking processes, has been relatively less explored. This inner-sphere reaction paradigm allows for a catalytic process where a single transition metal center participates in both photoexcitation and substrate activation steps (Scheme 1A). As such, an inner-sphere mechanism eliminates the need for an exogenous photosensitizer and holds the potential for reactivity and selectivity control through the metal center or ancillary ligands.

Catalytic applications of the inner-sphere-based pathways have seen recent growth and have demonstrated how the close interplay between the transition metal and visible light can benefit important mechanistic steps.[2] Notable examples include excited-state homolysis of M−R bond (e.g., M = Ni,[3] Cu,[4] Mo,[5] Pd,[6] Ce[7]) to generate an R• (e.g., alkyl, aryl, carboxylate, alkoxide, Cl) radical intermediate, activation of alkyl halides by photoexcited Pd[0],[8] and ligand- or metal-based control of enantioselectivity.[9] Despite such advantages of visible-light inner-sphere catalysis and its growing mechanistic insights,[3,7b,10] there are still numerous unanswered questions regarding the complex roles of transition metal in these reactions. Consequently, detailed characterization on the catalytic mechanism, particularly on the photoexcitation and substrate activation steps, will have important implications for the field of visible-light transition metal catalysis.[2]
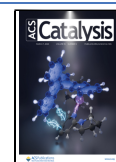
Our fundamental interest in the mechanistic understanding and reaction development of light-driven inner-sphere catalysis led us to investigate the catalytic dechlorination of trichloroacetic acid as the target transformation. Trichloroacetic acid

Scheme 1. General Reaction Schemes for Visible-Light Transition Metal Catalysis via an Inner-Sphere Mechanism and Previous Examples on Light-Driven Cu Catalysis with Carboxylic Acids

(A) Visible-Light Transition Metal Catalysis via an Inner-Sphere Mechanism
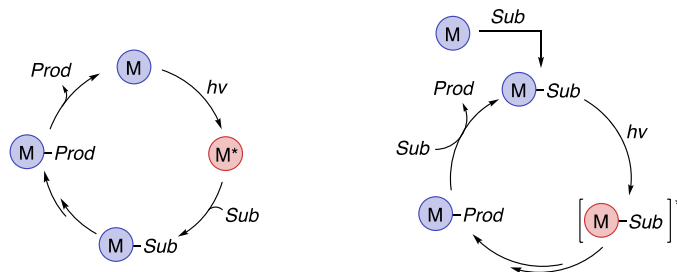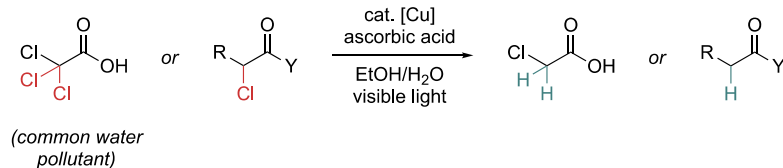
• Transition metal participates in both photoexcitation and substrate activation.

(B) Visible-Light-Driven, Cu-Catalyzed Decarboxylative Reactions (Ritter / Yoon / MacMillan)

(R = alkyl, aryl)   (ref. 4b–4d)   LMCT State
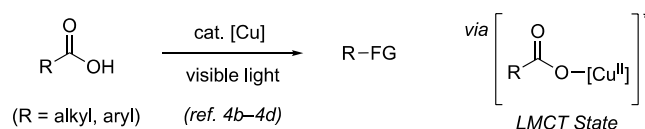
(C) *This Work: Visible-Light-Driven, Cu-Catalyzed Reductive Dehalogenation*

(common water pollutant)

• Dehalogenation over decarboxylation   • Halocarboxylic acids and -amides as substrates
• Enviromentally friendly conditions   • Copper's role in photoexcitation and C–Cl cleavage
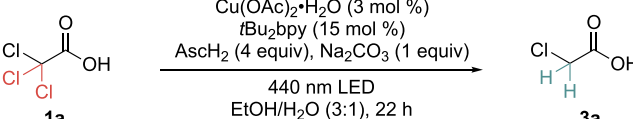
(TCA) is a common disinfection byproduct detected in drinking water[11] that is suspected to cause carcinogenic, mutagenic, and embryotoxic health effects.[12] For these reasons, efficient degradation of TCA is a highly desirable process and has received considerable amount of research interest.[13] TCA dechlorination methods based on electroreduction,[14] chemical reductants,[15] as well as UV-light-mediated examples[16] have been reported. While many of these examples show outstanding efficiency in TCA consumption, a mixture of products is often obtained. A visible-light-based catalytic dechlorination method has yet to be reported but finds its basis in the photoinduced cleavage of C–X (halogen) bonds in alkyl halides,[17] including C–X bonds in CX_3 groups.[18,19] Specifically, copper is well suited for light-driven C–X cleavage due to its established success in halogen atom transfer[20] and more recently, visible light catalysis.[4,21]

In visible-light-driven Cu catalysis with carboxylic acids, several recent reports have featured decarboxylative transformations (Scheme 1B). The key step of the mechanism involves the generation of a C-centered radical via CO_2 loss from the ligand-to-metal charge-transfer (LMCT) excited state of Cu^{II}-carboxylate species.[4b–d] We hypothesized that this potential side reaction could be mitigated under reductive dechlorination conditions, where the Cu^{II} species is reduced to Cu^I as the resting state, favoring C-halogen bond activation over decarboxylation.

Herein, we report a Cu-catalyzed, visible-light-driven dechlorination method of trichloroacetic acid that selectively forms monochloroacetic acid (Scheme 1C). The catalytic method can be further applied to other α-halocarboxylic acids and amides. Mechanistic studies have revealed the multiple roles of Cu in three key steps of the reaction: (i) photoexcitation; (ii) excited-state chlorine transfer; and (iii) thermal activation of C–Cl bond.

■ MATERIALS AND METHODS

Our initial optimization efforts on light-driven, Cu-catalyzed dechlorination of trichloroacetic acid (TCA, **1a**) revealed bipyridine ligands as the most effective ligand class, and its high modularity and easy access set an important foundation for conducting systematic mechanistic studies. Upon further screening, selective formation of monochloroacetic acid (MCA, **3a**) was observed under the optimal conditions featuring 4,4′-di-*tert*-butyl-2,2′-bipyridine (*t*Bu$_2$bpy) as the ancillary ligand, ascorbic acid (AscH$_2$) as the hydrogen atom source, and Na$_2$CO$_3$ as the base (Table 1). Control experiments indicate that Cu, light, and base were all essential for MCA formation (Table 1, entries 6, 8, and 10). The high selectivity for C–Cl bond cleavage in TCA contrasts with many recent examples of light-driven, Cu-catalyzed decarboxylative reactions,[4b−d] which was attributed to the fact that Cu^{II} carboxylate, the major species responsible for decarboxylation,

Table 1. Reaction Optimization for Light-Driven Dechlorination of TCA[a]

entry	change to standard condition	3a (%)
1	-	>99
2	CuCl instead of Cu(OAc)$_2$	<1
3	bpy as ligand	62
4	10% tBu$_2$bpy	77
5	iPrOH/H$_2$O (3:1) as solvent	72
6	no Cu(OAc)$_2$	<1
7	no tBu$_2$bpy	<1
8	no light	<1
9	no AscH$_2$	<1
10	no Na$_2$CO$_3$	<1

[a]Conditions beyond those indicated in the scheme: 1a (0.12 mmol), 1 mL solvent, under N$_2$ with irradiation from one 40 W Kessil lamp. Yields were determined by ^{1}H NMR analysis (relative to an internal standard). ^{t}Bu$_2$bpy: 4,4′-di-*tert*-butyl-2,2′-bipyridine. AscH$_2$: L-ascorbic acid. bpy: 2,2′-bipyridine.

was not formed under the reductive dechlorination conditions. The requirement of a relatively high tBu$_2$bpy-to-Cu ratio (≥5:1) (Figure S1) was attributed to the formation of [(tBu$_2$bpy)$_2$Cu]$^+$ as the active species, and its presence was later supported by results from UV/vis studies (*vide infra*). The excess amount of tBu$_2$bpy drives the complete formation of [(tBu$_2$bpy)$_2$Cu]$^+$ in the presence of other potential ligands, such as carboxylate or ascorbate. The dehydroascorbic acid byproduct likely underwent further degradation to form compounds such as oxalates,[22] which was supported through the isolation of a Cu-oxalate compound (7, Figure 1) characterized by X-ray crystallography (CCDC 2409532). Finally, the optimized reaction conditions feature a mixture of water/ethanol, an environmentally preferred green solvent system.[23]

We then went on to investigate the generality of the developed dechlorination method and whether the observed selectivity with 1a is retained with other substrates (Table 2). A range of carboxylic acids, esters, and amides (including primary, secondary, and tertiary) underwent efficient dechlorination under the optimized condition. The selective formation of monohalogenated product was observed with the ester, primary amide, and tribromoacetic acid substrate (1b–1d), achieving high-yielding conversion of pollutant molecules into synthetically useful α-halocarbonyl compounds.[24] Intrigued by the origin of the selectivity, we hypothesized that the third C−halogen bond cleavage may be sluggish due to the formation of

an unstable primary C-centered radical, and such a challenge can be addressed if a secondary or a benzylic radical is formed instead. Indeed, chlorocarbonyl compounds containing an α-alkyl or α-phenyl substituent underwent successful dechlorination, and moderate to good yields were obtained for carboxylic acids (3e, 3f), secondary amides (3g–3n), and tertiary amides (3o, 3p), including N-pyridyl (3l) and cyclic (3n) amides. Notably, the dechlorination was selective for C(sp^3)−Cl bonds, as the chlorophenyl group in 1m remained intact under the reaction condition. The reaction yields are generally higher with N-aryl-substituted amides (3m), which may originate from further stabilization of the radical intermediate through conjugation. The successful dechlorination of amides containing a secondary or benzylic C−Cl bond not only supports the intermediacy of the α-carbonyl radical in the reaction mechanism but also represents an efficient method for the degradation of α-chloroamides, a related class of organic halide pollutants.[25]

Spectroscopic studies were carried out to gain insights into the ground-state speciation of Cu before light irradiation (Scheme 2). The UV/vis spectrum of the reaction mixture, obtained under N$_2$, features a dominant band at ~440 nm (Scheme 2B, 0 h). The position of this band is at a similar region to the one reported for Cu(bpy)$_2$$^+$ (437 nm, EtOH/MeOH 4:1), which was assigned to Cu^I to bpy charge transfer.[26] During optimization studies, a higher yield of 3a was observed with light irradiation at 440 nm than at 390 nm (Table S2). Along with the beneficial effect of high ligand loading (cf. Table 1, and Figure S1), we propose [(tBu$_2$bpy)$_2$Cu]$^+$ (4) as the major Cu species in the system and the photoactive species. The presence of [(tBu$_2$bpy)$_2$Cu]$^+$ was further confirmed by X-ray crystallographic characterization of a red-brown crystal formed from the reaction condition (Scheme 2A), and the structure was determined as [(tBu$_2$bpy)$_2$Cu][CuCl$_2$] (4a) by X-ray crystallography (CCDC 2409530).[27]

Further insights into the Cu speciation under the reaction conditions have been obtained from UV/vis studies of the reaction mixture after light irradiation (Scheme 2B). The spectra indicate that the species at ~440 nm, [(tBu$_2$bpy)$_2$Cu]$^+$ (4), persisted as the major species after 2−10 h irradiation. In addition, the concentration of this species gradually decreased over time, while a new band at ~750 nm concomitantly arose, suggesting the formation of a new Cu species during the reaction. The position of the new band was consistent with the d-d transition commonly observed for Cu^{II} species. This was tentatively assigned as a (tBu$_2$bpy)$_2$Cu^{II}X$_n$ species (n = 1 or 2, X = Cl or carboxylate) formed from excited-state chlorine atom transfer, based on the similar position of the absorbance reported for (bpy)$_2$Cu^{II}X$_2$ (740 nm).[20] Once a Cu−Cl bond is formed, the chloride may undergo facile exchange with
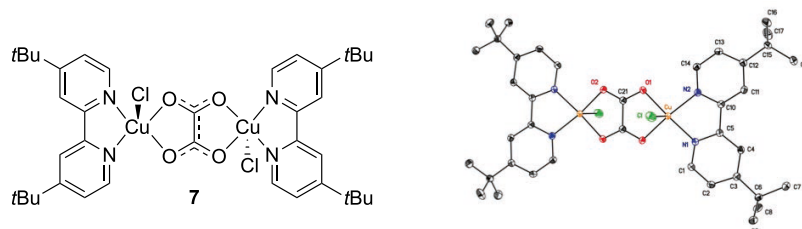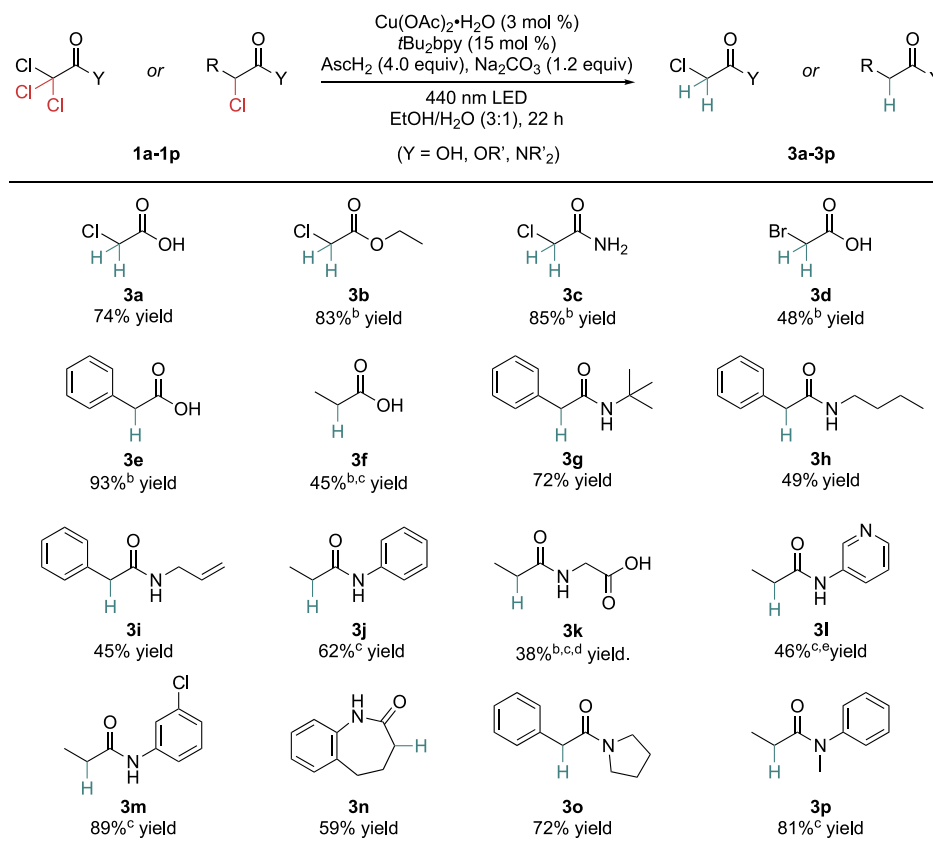

Figure 1. Structure of Cu-oxalate isolated from light-driven dechlorination.

Table 2. Substrate Scope of Light-Driven Dehalogenation[a]

Reaction scheme:

Cl₃C(O)Y (dichloro/trichloro acetyl) or R–CHCl–C(O)Y **1a–1p**

Cu(OAc)₂·H₂O (3 mol %), tBu₂bpy (15 mol %), AscH₂ (4.0 equiv), Na₂CO₃ (1.2 equiv), 440 nm LED, EtOH/H₂O (3:1), 22 h

→ ClCH₂C(O)Y or R–CH₂–C(O)Y **3a–3p**   (Y = OH, OR′, NR′₂)

3a	3b	3c	3d
74% yield	83%[b] yield	85%[b] yield	48%[b] yield
3e	3f	3g	3h
93%[b] yield	45%[b,c] yield	72% yield	49% yield
3i	3j	3k	3l
45% yield	62%[c] yield	38%[b,c,d] yield.	46%[c,e] yield
3m	3n	3o	3p
89%[c] yield	59% yield	72% yield	81%[c] yield

[a]Standard reaction conditions: Halogenated substrate (0.12 mmol), ascorbic acid (4.0 equiv), Na₂CO₃ (1.2 equiv), Cu(OAc)₂(H₂O) (3 mol %), 4,4′-di-tert-butyl-2,2′-bipyridine (15 mol %), EtOH/H₂O (3:1 v/v, 1.0 mL), N₂, 440 nm LED, room temperature, 22 h. Isolated yields. [b]Yields are calculated from ¹H NMR analysis with DMF as the internal standard. [c]Cu(OAc)₂·H₂O (20 mol %), 4,4′-di-tert-butyl-2,2′-bipyridine (100 mol %). [d]Substrate (0.24 M). [e]Na₂CO₃ (2.5 equiv).

carboxylate (e.g., dichloroacetate).[28] Further evidence for chlorine transfer to Cu[I] was obtained by isolation of a blue compound from the reaction mixture, and its structure was subsequently established by X-ray crystallography as [(tBu₂bpy)CuCl][CuCl₂] (5a, CCDC 2409531).[27] While we cannot rule out the possibility that the new UV/vis band arises from a different Cu[II] species, the characterization of [(tBu₂bpy)₂Cu[I]]⁺ and [(tBu₂bpy)₂Cu[II]Cl]⁺ under the reaction conditions provided strong evidence for a Cu-based excited-state chlorine transfer step in the catalytic mechanism.

Next, we probed whether excited-state chlorine transfer was the mechanism for both C−Cl cleavage steps from TCA. While conducting optimization studies, we noted that the dichloro-acetic acid (DCA, 2a) was formed even in the absence of visible light irradiation (Table S1). This observation was consistent with our later discovery that mixing Cu(OAc)₂, ligand, and TCA under ambient conditions yielded a new Cu species, and the structure was determined as (tBu₂bpy)-Cu[II](Cl)(dichloroacetate) (6) by X-ray crystallography (Scheme 3, CCDC 2409529). While the detailed mechanism of its formation is still under investigation, the observation of such species provided evidence for a ground-state cleavage of the first C−Cl bond in TCA. Collectively, the speciation studies described above suggested that the first C−Cl cleavage in TCA was thermally driven, while the second C−Cl cleavage was through a light-driven chlorine atom transfer with [(tBu₂bpy)Cu[I]]⁺.

The characterization of Cu speciation in the reaction mixture led us to further probe the nature of the turnover-limiting steps in the catalytic mechanism. The reaction time course of product 3a formation was monitored by NMR at 30 min intervals after the start of light irradiation. Catalytic dechlorination of TCA showed near-quantitative formation of DCA within 30 min in the absence of light, consistent with thermally driven first C−Cl cleavage as suggested by the stoichiometric studies (cf. Scheme 3). Upon light irradiation, DCA consumption was observed concurrently with MCA formation at a similar rate. Notably, the time courses and reaction rates were nearly identical to those obtained using DCA directly as the substrate (Figure S6). These observations suggested that under the catalytic conditions, the first C−Cl cleavage took place in the absence of light and formed DCA, which exhibited a much higher rate than the second C−Cl cleavage for MCA formation.

To gain deeper insights into the excited-state C−Cl cleavage step, the rate of catalytic dechlorination of DCA was determined using different bipyridine ligands bearing electroni-cally varied 4,4′-substituent (R). Plotting the reaction rate against the Hammett parameter of R[29] (Figure 2A) revealed similar performance with electron-rich bipyridines (R = OMe, tBu) but significantly decreased rates with the unsubstituted and brominated bipyridine, suggesting that an electron-rich Cu is crucial for efficient catalytic dechlorination. The origin of the H atoms in the MCA product was probed through a deuterium

Scheme 2. Characterization of $[(tBu_2bpy)_2Cu^I]$ and $[(tBu_2bpy)_2Cu^{II}Cl]$ Species[a]
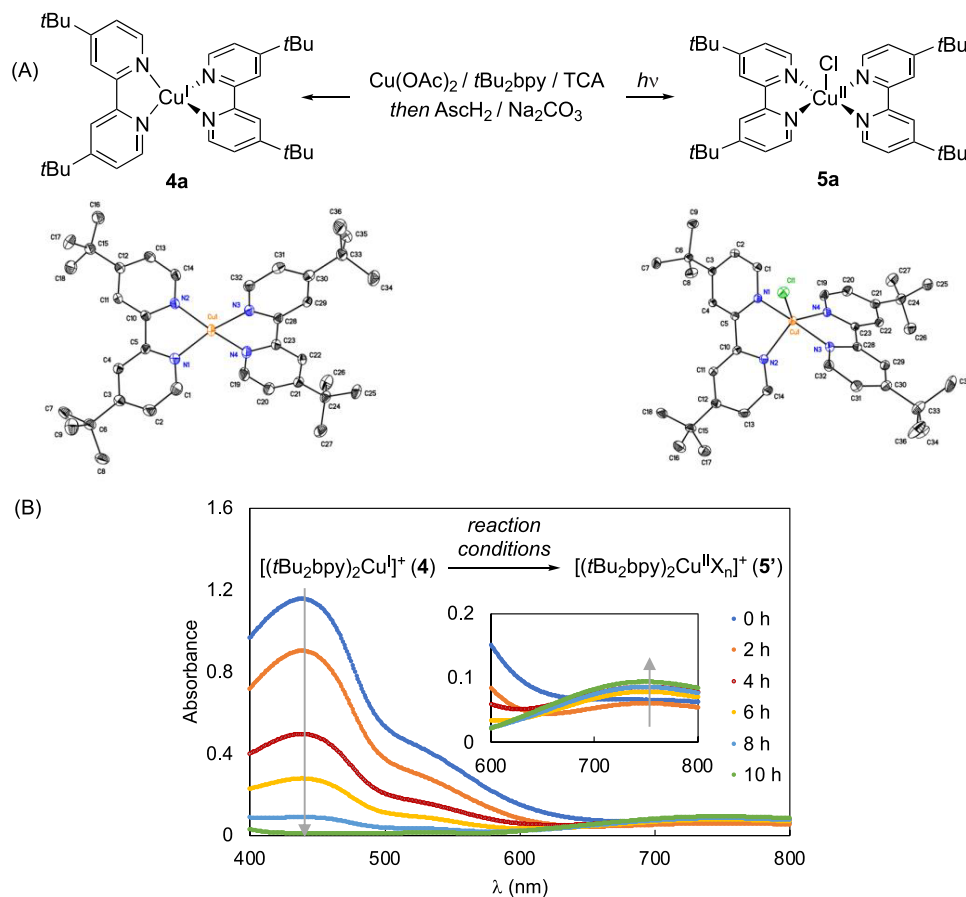
[a]Conditions: (A) Formation of 4a: Cu(OAc)$_2$, tBu$_2$bpy (2.5 equiv), TCA (4 equiv), then ascH$_2$ (16 equiv), Na$_2$CO$_3$ (4 equiv), N$_2$, 2 d; 5a: Cu(OAc)$_2$, tBu$_2$bpy (2.5 equiv), TCA (4 equiv), then ascH$_2$ (16 equiv), Na$_2$CO$_3$ (4 equiv), 440 nm LED, N$_2$, 30 min, then light off, 2 d; the CuCl$_2^-$ counterion in 4a and 5a is not shown. (B) TCA (0.03 M), Cu(OAc)$_2$ (2 mol %), tBu$_2$bpy (14 mol %), Na$_2$CO$_3$ (1 equiv), ascH$_2$ (4 equiv), EtOH/H$_2$O (3:1) (4 mL), N$_2$, 440 nm LED.

Scheme 3. Cu−Mediated First C−Cl Cleavage in TCA
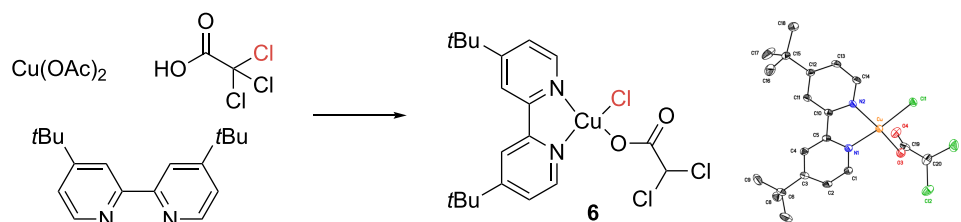
incorporation experiment. Catalytic dechlorination with ascorbic acid-d_4 led to the formation of deuterated DCA and MCA, determined by ^{2}H NMR spectroscopy (Figure 2B and Table S6, deuterated solvents were used to prevent rapid proton exchange between ascorbic acid enol OH and solvents).[30] These results, combined with thermodynamic data that the O−H bonds in AscH$_2$, are significantly weaker (69−75 kcal/mol) than those in alcohol or water (>100 kcal/mol),[31,32] provided strong support that the C−H bonds in the MCA product were formed through hydrogen atom transfer from AscH$_2$.

The mechanistic studies described above allowed us to propose a mechanism for the Cu-catalyzed, visible-light-driven dechlorination reaction (Figure 3). Under the optimized reaction conditions (TCA/Na$_2$CO$_3$/AscH$_2$ ~1:1:4), both TCA

(pK_a = 0.65)[33] and 1 equiv of AscH$_2$ (pK_a = 4.0, 11.3)[31] are deprotonated by Na$_2$CO$_3$ (pK_a = 6.35, 10.33)[33] to form trichloroacetate and AscH$^-$ (O−H bond dissociation free energy = 68.6 kcal/mol), a more potent hydrogen atom donor than AscH$_2$ (O−H BDFE = 74.9 kcal/mol).[31] Based on literature data with similar chlorinated organic compounds[34] and reported trend for CCl$_4$, CHCl$_3$, and CH$_2$Cl$_2$,[35] we expect the BDFE of the C−Cl bonds in TCA to be ~70 kcal/mol and those in DCA and MCA to be 5−10 kcal/mol higher. The trend here is consistent with the observed reactivity difference, where light irradiation is only essential for the second C−Cl cleavage of TCA.

The mechanism of light-driven dechlorination [Figure 3, part (ii)] starts with the formation of $[(tBu_2bpy)Cu^I]^+$ (4) as the photoactive species. Upon irradiation at 440 nm, species 4

(A) Hammett Studies:
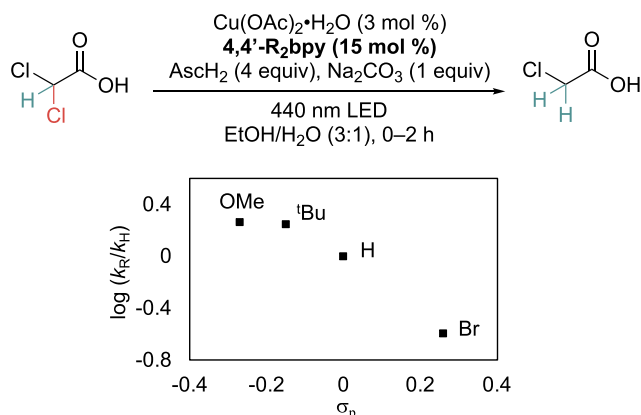
(B) Deuterium Incorporation:
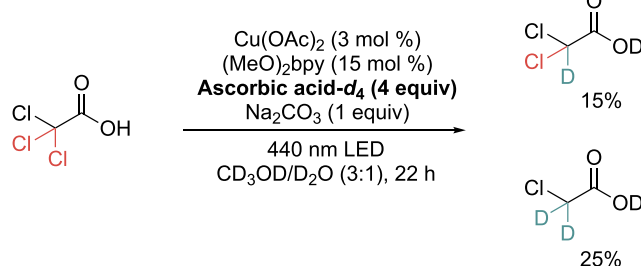

Figure 2. Mechanistic studies: (A) Dependence of the reaction rate on bipyridine ligands. Conditions: DCA (0.23 M), Cu(OAc)$_2$·H$_2$O (3 mol %), 4,4′-disubstituted-2,2′-bipyridine (15 mol %, R = OMe, tBu, H, or Br), ascorbic acid (4 equiv), Na$_2$CO$_3$ (1.2 equiv), EtOH/H$_2$O (3:1 v/v, 1 mL), DMF (5.0 μL, internal standard), 440 nm LED, N$_2$. (B) Deuterium incorporation studies. Conditions: TCA (0.12 M), Cu(OAc)$_2$ (3 mol %), 4,4′-dimethoxy-2,2′-bipyridine (15 mol %), ascorbic acid-d_4 (4 equiv), Na$_2$CO$_3$ (1.2 equiv), CD$_3$OD/D$_2$O (3:1 v/v, 1 mL), C$_6$D$_6$ (5.0 μL, internal standard), 440 nm LED, N$_2$.

reaches the metal-to-ligand charge-transfer (MLCT) state **4***[26] and undergoes subsequent chlorine transfer with deprotonated DCA (pK_a = 1.29)[33] to form the Cu^{II}−Cl intermediate **5** and a C-centered α radical.[36] We propose chlorine transfer as the turnover-limiting step. This may occur either as a direct chlorine atom transfer[10b] or as a single electron reduction of dichloroacetate ($E^{RX/R•}$ ∼ − 0.6 V vs SCE)[37] by excited-state [(tBu$_2$bpy)Cu^I]$^+$ ($E^{II/I*}$ ∼ − 1.23 V vs SCE)[21b] followed by Cl$^-$ binding to Cu^{II}. Both the concerted and stepwise pathways could benefit from a more electron-rich Cu center, with the same electronic dependence as the observed Hammett correlation (cf. Figure 2A). In addition, radical formation as the turnover-limiting step is consistent with the higher yields obtained with benzylic and secondary alkyl substrates in the scope studies (cf. Table 2). The subsequent HAT step between ascorbate (O−H BDFE = 68.6 kcal/mol) and α radical (C−H BDFE ∼ 90−100 kcal/mol)[35,38] is largely exergonic and should be relatively facile. Finally, the Cu^{II} intermediate is reduced by the ascorbate radical anion to form the Cu^I active catalyst and the dehydroascorbic acid byproduct.

CONCLUSIONS

In conclusion, we have developed a visible-light-driven, Cu-catalyzed dehalogenation method for halocarboxylic acids and amides. This catalytic reaction employs ascorbic acid and ethanol/water as environmentally friendly stoichiometric reductant and solvent that selectively converts trichloroacetic

(i) Formation of dichloroacetate under thermal conditions:
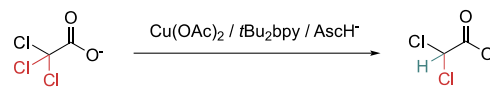
(ii) Visible-light-driven dechlorination:
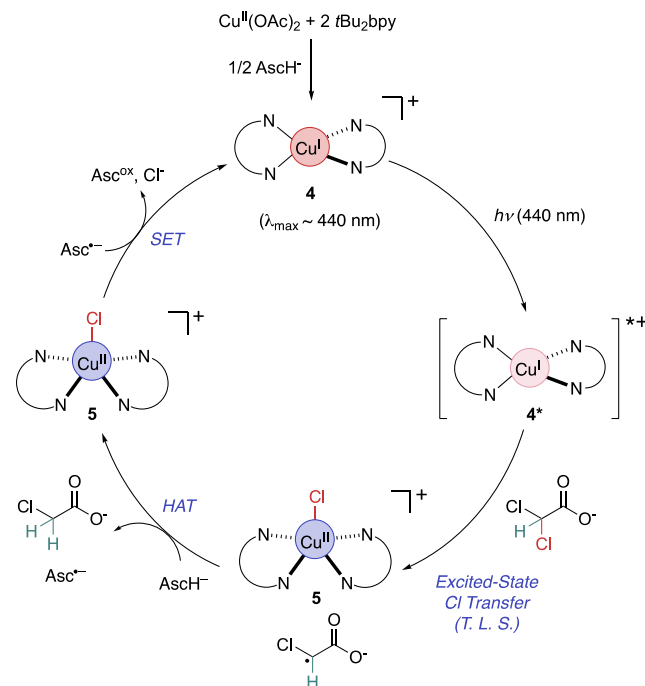
Figure 3. Proposed mechanism for the catalytic dechlorination of TCA to MCA. AscH$_2$: ascorbic acid; AscH$^-$: ascorbate; Asc$^{•-}$: ascorbate radical anion; Asc^{ox}: dehydroascorbic acid; HAT: hydrogen atom transfer; SET: single electron transfer; T.L.S.: turnover-limiting step.

acid, a pollutant molecule, into synthetically useful mono-chloroacetic acid. Efficient dehalogenation of a wide range of α-halocarboxylic acids and amides has also been achieved using the catalytic method. Combined spectroscopic and kinetic studies have provided mechanistic insights into the catalytic reaction, which disclosed the multiple roles of copper in photoexcitation, thermal activation of the first C−Cl bond, and excited-state chlorine transfer with the second C−Cl bond. The catalytic dehalogenation method exhibits orthogonal chemoselectivity to several recent reports on Cu-catalyzed, visible-light-driven decarboxylative reactions,[4b−d] which is attributed to Cu^I as the resting state under reductive conditions. Further studies on dehalogenative reactions are currently being conducted in our laboratory to extend the synthetic utility and mechanistic understanding of the complex roles of transition metal in visible-light-driven, inner-sphere catalysis.

ASSOCIATED CONTENT

Supporting Information

The Supporting Information is available free of charge at https://pubs.acs.org/doi/10.1021/acscatal.4c07845.

Additional experimental details, materials, methods (including photographs of experimental setup), characterization, and spectral information (PDF)
Crystallographic data for **4a** (CIF)
Crystallographic data for **5a** (CIF)

Crystallographic data for **6** (CIF)
Crystallographic data for **7** (CIF)

■ AUTHOR INFORMATION

Corresponding Author

Dian Wang − *Department of Chemistry, Marquette University, Milwaukee, Wisconsin 53201, United States;* ● orcid.org/0000-0001-9965-4079; Email: dian.wang@marquette.edu

Authors

Abigail J. Thillman − *Department of Chemistry, Marquette University, Milwaukee, Wisconsin 53201, United States*

Erin C. Kill − *Department of Chemistry, Marquette University, Milwaukee, Wisconsin 53201, United States*

Alexander N. Erickson − *Department of Chemistry, Marquette University, Milwaukee, Wisconsin 53201, United States;* ● orcid.org/0009-0007-5837-0978

Complete contact information is available at:
https://pubs.acs.org/10.1021/acscatal.4c07845

Author Contributions

The manuscript was written through contributions of all authors. All authors have given approval to the final version of the manuscript.

Notes

The authors declare no competing financial interest.

■ ACKNOWLEDGMENTS

■ ABBREVIATIONS

TCA, trichloroacetic acid; DCA, dichloroacetic acid; MCA, monochloroacetic acid; LMCT, ligand-to-metal charge transfer; MLCT, metal-to-ligand charge transfer; SCE, saturated calomel electrode; BDFE, bond dissociation free energy; HAT, hydrogen atom transfer; SET, single electron transfer; T.L.S., turnover-limiting step

■ REFERENCES

(1) (a) *Visible Light Photocatalysis in Organic Chemistry*; Stephenson, C. R. J.; Yoon, T. P.; MacMillan, D. W. C., Eds.; Wiley: Hoboken, NJ, 2018. (b) Strieth-Kalthoff, F.; James, M. J.; Teders, M.; Pitzer, L.; Glorius, F. Energy transfer catalysis mediated by visible light: principles, applications, directions. *Chem. Soc. Rev.* **2018**, *47*, 7190−7202. (c) Glaser, F.; Kerzig, C.; Wenger, O. S. Multi-Photon Excitation in Photoredox Catalysis: Concepts, Applications Methods. *Angew. Chem. Int. Ed.* **2020**, *59*, 10266−10284. (d) Yu, X. Y.; Chen, J. R.; Xiao, W. J. Visible Light-Driven Radical-Mediated C-C Bond Cleavage/Functionalization in Organic Synthesis. *Chem. Rev.* **2021**, *121*, 506−561. (e) Chan, A. Y.; Perry, I. B.; Bissonnette, N. B.; Buksh, B. F.; Edwards, G. A.; Frye, L. I.; Garry, O. L.; Lavagnino, M. N.; Li, B. X.; Liang, Y.; Mao, E.; Millet, A.; Oakley, J. V.; Reed, N. L.; Sakai, H. A.; Seath, C. P.; MacMillan, D. W. C. Metallaphotoredox: The Merger of Photoredox and Transition Metal Catalysis. *Chem. Rev.* **2022**, *122*, 1485−1542. (f) Holmberg-Douglas, N.; Nicewicz, D. A. Photoredox-Catalyzed C-H Functionalization Reactions. *Chem. Rev.* **2022**, *122*, 1925−2016. (g) Pitre, S. P.; Overman, L. E. Strategic Use of Visible-Light Photoredox Catalysis in Natural Product Synthesis. *Chem. Rev.* **2022**, *122*, 1717−1751. (h) Li, J.; Zhang, D.; Hu, Z. Ligand-Enabled "Two-in-One" Metallaphotocatalytic Cross Couplings. *ACS Catal.* **2025**, *15*, 1635−1654.

(2) For a leading review, see: Cheung, K. P. S.; Sarkar, S.; Gevorgyan, V. Visible Light-Induced Transition Metal Catalysis. *Chem. Rev.* **2022**, *122*, 1543−1625.

(3) (a) Ting, S. I.; Garakyaraghi, S.; Taliaferro, C. M.; Shields, B. J.; Scholes, G. D.; Castellano, F. N.; Doyle, A. G. ^{3}d-d Excited States of Ni(II) Complexes Relevant to Photoredox Catalysis: Spectroscopic Identification and Mechanistic Implications. *J. Am. Chem. Soc.* **2020**, *142*, 5800−5810. (b) Cagan, D. A.; Stroscio, G. D.; Cusumano, A. Q.; Hadt, R. G. Multireference Description of Nickel-Aryl Homolytic Bond Dissociation Processes in Photoredox Catalysis. *J. Phys. Chem. A* **2020**, *124*, 9915−9922.

(4) (a) Treacy, S. M.; Rovis, T. Copper Catalyzed C(sp^3)- H Bond Alkylation via Photoinduced Ligand-to-Metal Charge Transfer. *J. Am. Chem. Soc.* **2021**, *143*, 2729−2735. (b) Xu, P.; Lopez-Rojas, P.; Ritter, T. Radical Decarboxylative Carbometalation of Benzoic Acids: A Solution to Aromatic Decarboxylative Fluorination. *J. Am. Chem. Soc.* **2021**, *143*, 5349−5354. (c) Li, Q. Y.; Gockel, S. N.; Lutovsky, G. A.; DeGlopper, K. S.; Baldwin, N. J.; Bundesmann, M. W.; Tucker, J. W.; Bagley, S. W.; Yoon, T. P. Decarboxylative cross-nucleophile coupling via ligand-to-metal charge transfer photoexcitation of Cu(II) carboxylates. *Nat. Chem.* **2022**, *14*, 94−99. (d) Dow, N. W.; Pedersen, P. S.; Chen, T. Q.; Blakemore, D. C.; Dechert-Schmitt, A. M.; Knauber, T.; MacMillan, D. W. C. Decarboxylative Borylation and Cross-Coupling of (Hetero)aryl Acids Enabled by Copper Charge Transfer Catalysis. *J. Am. Chem. Soc.* **2022**, *144*, 6163−6172.

(5) Fosshat, S.; Siddhiaratchi, S. D. M.; Baumberger, C. L.; Ortiz, V. R.; Fronczek, F. R.; Chambers, M. B. Light-Initiated C-H Activation via Net Hydrogen Atom Transfer to a Molybdenum(VI) Dioxo. *J. Am. Chem. Soc.* **2022**, *144*, 20472−20483.

(6) Waddell, P. M.; Tian, L.; Scavuzzo, A. R.; Venigalla, L.; Scholes, G. D.; Carrow, B. P. Visible light-induced palladium-carbon bond weakening in catalytically relevant T-shaped complexes. *Chem. Sci.* **2023**, *14*, 14217−14228.

(7) (a) Hu, A. H.; Guo, J. J.; Pan, H.; Tang, H. M.; Gao, Z. B.; Zuo, Z. W. δ-Selective Functionalization of Alkanols Enabled by Visible-Light-Induced Ligand-to-Metal Charge Transfer. *J. Am. Chem. Soc.* **2018**, *140*, 1612−1616. (b) Yang, Q. M.; Wang, Y. H.; Qiao, Y. S.; Gau, M.; Carroll, P. J.; Walsh, P. J.; Schelter, E. J. Photocatalytic C-H activation and the subtle role of chlorine radical complexation in reactivity. *Science* **2021**, *372*, 847−852.

(8) (a) Parasram, M.; Chuentragool, P.; Sarkar, D.; Gevorgyan, V. Photoinduced Formation of Hybrid Aryl Pd-Radical Species Capable of 1,5-HAT: Selective Catalytic Oxidation of Silyl Ethers into Silyl Enol Ethers. *J. Am. Chem. Soc.* **2016**, *138*, 6340−6343. (b) Torres, G. M.; Liu, Y.; Arndtsen, B. A. A dual light-driven palladium catalyst: Breaking the barriers in carbonylation reactions. *Science* **2020**, *368*, 318−323. (c) Zhao, G. Y.; Yao, W.; Mauro, J. N.; Ngai, M. Y. Excited-State Palladium-Catalyzed 1,2-Spin-Center Shift Enables Selective C-2 Reduction, Deuteration, and Iodination of Carbohydrates. *J. Am. Chem. Soc.* **2021**, *143*, 1728−1734.

(9) (a) Kainz, Q. M.; Matier, C. D.; Bartoszewicz, A.; Zultanski, S. L.; Peters, J. C.; Fu, G. C. Asymmetric copper-catalyzed C-N cross-couplings induced by visible light. *Science* **2016**, *351*, 681−684. (b) Skubi, K. L.; Kidd, J. B.; Jung, H.; Guzei, I. A.; Baik, M. H.; Yoon, T. P. Enantioselective Excited-State Photoreactions Controlled By A Chiral Hydrogen-Bonding Iridium Sensitizer. *J. Am. Chem. Soc.* **2017**, *139*, 17186−17192. (c) Steinlandt, P. S.; Zhang, L.; Meggers, E. Metal Stereogenicity in Asymmetric Transition Metal Catalysis. *Chem. Rev.* **2023**, *123*, 4764−4794.

(10) (a) Park, Y.; Kim, S.; Tian, L.; Zhong, H.; Scholes, G. D.; Chirik, P. J. Visible light enables catalytic formation of weak chemical bonds with molecular hydrogen. *Nat. Chem.* 2021, *13*, 969−976. (b) Pham, L. N.; Olding, A.; Ho, C. C.; Bissember, A. C.; Coote, M. L. Investigating Competing Inner- and Outer-Sphere Electron-Transfer Pathways in Copper Photoredox-Catalyzed Atom-Transfer Radical Additions: Closing the Cycle. *Angew. Chem., Int. Ed.* 2025, *64*, No. e202415792. (c) Tang, R.; Wan, Q.; Lam, T.-L.; To, W.-P.; Low, K.-H.; Tang, Z.; Du, L.; Lu, W.; Che, C.-M. Copper(I)-based metal-metal-to-ligand charge transfer excited state with halogen-atom transfer photo-reactivity and photocatalysis. *Chem* 2024, *10*, 2807−2828.

(11) (a) Christman, R. F.; Norwood, D. L.; Millington, D. S.; Johnson, J. D.; Stevens, A. A. Identity and yields of major halogenated products of aquatic fulvic acid chlorination. *Environ. Sci. Technol.* 1983, *17*, 625−628. (b) Hong, Y.; Song, H.; Karanfil, T. Formation of haloacetic acids from dissolved organic matter fractions during chloramination. *Water. Res.* 2013, *47*, 1147−1155.

(12) Wang, W.; Ye, B.; Yang, L.; Li, Y.; Wang, Y. Risk assessment on disinfection by-products of drinking water of different water sources and disinfection processes. *Environ. Int.* 2007, *33*, 219−225.

(13) For leading reviews, see: (a) Ilunga, A. K.; Mamba, B. B.; Nkambule, T. T. I. Catalytic hydrodehalogenation of halogenated disinfection byproducts for clean drinking water production: A review. *J. Water Process Eng.* 2021, *44*, No. 102402. (b) Li, J.; Zhang, C.; Li, Y.; Pan, Y.; Liu, Y. Rational Design and Structural Regulation of Robust Catalysts for Electrocatalytic Hydrodechlorination: From Nanostructures to Single Atoms. *ACS Catal.* 2023, *13*, 9633−9655.

(14) (a) Rusling, J. F.; Miaw, C. L.; Couture, E. C. Electrocatalytic Dehalogenation of Alpha-Haloacetic Acids by Vitamin-B12. *Inorg. Chem.* 1990, *29*, 2025−2027. (b) Mao, R.; Li, N.; Lan, H.; Zhao, X.; Liu, H.; Qu, J.; Sun, M. Dechlorination of Trichloroacetic Acid Using a Noble Metal-Free Graphene-Cu Foam Electrode via Direct Cathodic Reduction and Atomic H. *Environ. Sci. Technol.* 2016, *50*, 3829−3837. (c) Liu, Y.; Mao, R.; Tong, Y.; Lan, H.; Zhang, G.; Liu, H.; Qu, J. Reductive dechlorination of trichloroacetic acid (TCAA) by electrochemical process over Pd-In/Al₂O₃ catalyst. *Electrochim. Acta* 2017, *232*, 13−21. (d) Ma, X. Y.; Huang, S. N.; Jin, Y. H.; Jiang, H.; Tang, L. J.; Wu, Y. F.; Ni, Y. J.; Zhu, S. J.; Li, X. Y.; Dietrich, A. M. Electrocatalytic dechlorination of aqueous trichloroacetic acid by Vitamin B12 modified iron electrode. *J. Environ. Chem. Eng.* 2023, *11*, No. 109944.

(15) (a) Zhou, J.; Han, Y.; Wang, W.; Xu, Z.; Wan, H.; Yin, D.; Zheng, S.; Zhu, D. Reductive removal of chloroacetic acids by catalytic hydrodechlorination over Pd/ZrO₂ catalysts. *Appl. Catal., B* 2013, *134−135*, 222−230. (b) Neelam; Meyerstein, D.; Burg, A.; Shamir, D.; Albo, Y. Polyoxometalates entrapped in sol-gel matrices as electron exchange columns and catalysts for the reductive de-halogenation of halo-organic acids in water. *J. Coord. Chem.* 2018, *71*, 3180−3193. (c) Albo, Y.; Meyerstein, D.; Neelam Zero Valent Iron Catalyst for Reduction Processes. WO/155476A12019; August 15, 2019. (d) Nieto-Sandoval, J.; Gomez-Herrero, E.; El Morabet, F.; Munoz, M.; de Pedro, Z. M.; Casas, J. A. Catalytic Hydro-dehalogenation of Haloacetic Acids: A Kinetic Study. *Ind. Eng. Chem. Res.* 2020, *59*, 17779−17785. (e) Cai, Y.; Long, X.; Luo, Y. H.; Zhou, C.; Rittmann, B. E. Stable dechlorination of Trichloroacetic Acid (TCAA) to acetic acid catalyzed by palladium nanoparticles deposited on H₂-transfer membranes. *Water Res.* 2021, *192*, No. 116841.

(16) (a) Gan, J.; Zhu, T.; Zhang, Y.; Li, D.; Li, T.; Zhao, M.; Zhao, Z.; Wang, L. Degradation and dechlorination of trichloroacetic acid induced by an in situ 222 nm KrCl* excimer radiation. *Chemosphere* 2023, *331*, No. 138753. (b) Zhang, Q.; Wang, X.; Wu, N.; Zhu, C.; Qin, W.; Huang, D.; Zhou, D. Advanced reduction processes initiated by oxidative radicals for trichloroacetic acid degradation: Performance, radical generation, and mechanism. *Water Res.* 2025, *268*, No. 122587.

(17) For leading reviews, see: (a) Crespi, S.; Fagnoni, M. Generation of Alkyl Radicals: From the Tyranny of Tin to the Photon

Democracy. *Chem. Rev.* 2020, *120*, 9790−9833. (b) Juliá, F.; Constantin, T.; Leonori, D. Applications of Halogen-Atom Transfer (XAT) for the Generation of Carbon Radicals in Synthetic Photochemistry and Photocatalysis. *Chem. Rev.* 2022, *122*, 2292−2352. (c) Evano, G.; Theunissen, C. Copper-(Photo)Catalyzed Radical Reactions with Organic Halides. *Synlett* 2024, *35*, 485−499.

(18) See ref 17 and: (a) Giri, R.; Mosiagin, I.; Franzoni, I.; Notel, N. Y.; Patra, S.; Katayev, D. Photoredox Activation of Anhydrides for the Solvent-Controlled Switchable Synthesis of gem-Difluoro Compounds. *Angew. Chem., Int. Ed.* 2022, *61*, No. e202209143. (b) Singh, H.; Inaththappulige, S.; Tak, R. K.; Giri, R. α-Bromoacetate as a Mild and Safe Brominating Agent in the Light-Driven Vicinal Dibromination of Unactivated Alkenes and Alkynes. *Org. Lett.* 2024, *26*, 5478−5481. (c) Wang, J.; Gao, G.; Cheng, J.; Li, J.; Chen, X.; Chen, X.; Zhang, D.; Li, H.; Cai, X.; Huang, B. Photocatalytic organosulfur reagent-promoted selective mono-(deutero)-hydrodechlorination. *Green. Chem.* 2024, *26*, 5167−5172.

(19) For nonphotochemical C-halogen cleavage in CX₃-containing substrates, see ref 17a and: (a) Zhao, Q.; Li, B.; Zhou, X.; Wang, Z.; Zhang, F. L.; Li, Y.; Zhou, X.; Fu, Y.; Wang, Y. F. Boryl Radicals Enabled a Three-Step Sequence to Assemble All-Carbon Quaternary Centers from Activated Trichloromethyl Groups. *J. Am. Chem. Soc.* 2022, *144*, 15275−15285. (b) Bo, M. C.; Phang, Y. L.; Zhao, Q.; Zhang, F. L.; Wang, Y. F. Lewis Base-Boryl Radicals Promoted Selective Mono- and Di- Hydrodechlorination of Trichloroacetamides and Acetates. *Eur. J. Org. Chem.* 2024, *27*, No. e202301189.

(20) Peng, C.-H.; Kong, J.; Seeliger, F.; Matyjaszewski, K. Mechanism of Halogen Exchange in ATRP. *Macromolecules* 2011, *44*, 7546−7557.

(21) (a) Hossain, A.; Bhattacharyya, A.; Reiser, O. Copper's rapid ascent in visible-light photoredox catalysis. *Science* 2019, *364*, No. eaav9713. (b) Beaudelot, J.; Oger, S.; Perusko, S.; Phan, T. A.; Teunens, T.; Moucheron, C.; Evano, G. Photoactive Copper Complexes: Properties and Applications. *Chem. Rev.* 2022, *122*, 16365−16609. (c) Mukherjee, U.; Shah, J. A.; Ngai, M.-Y. Visible light-driven excited-state copper-BINAP catalysis for accessing diverse chemical reactions. *Chem. Catal.* 2024, *4*, No. 101184.

(22) (a) Khamespanah, F.; Marx, M.; Crochet, D. B.; Pokharel, U. R.; Fronczek, F. R.; Maverick, A. W.; Beller, M. Oxalate production via oxidation of ascorbate rather than reduction of carbon dioxide. *Nat. Commun.* 2021, *12*, No. 1997. (b) Ford, C. M.; Sweetman, C.; Fry, S. C. Ascorbate degradation: pathways, products, and possibilities. *J. Exp. Bot.* 2024, *75*, 2733−2739.

(23) (a) Capello, C.; Fischer, U.; Hungerbühler, K. What is a green solvent? A comprehensive framework for the environmental assessment of solvents. *Green. Chem.* 2007, *9*, 927−934. (b) Tekin, K.; Hao, N.; Karagoz, S.; Ragauskas, A. J. Ethanol: A Promising Green Solvent for the Deconstruction of Lignocellulose. *ChemSusChem* 2018, *11*, 3559−3575.

(24) Fantinati, A.; Zanirato, V.; Marchetti, P.; Trapella, C. The Fascinating Chemistry of α-Haloamides. *ChemistryOpen* 2020, *9*, 100−170.

(25) (a) Lou, Y.-Y.; Hapiot, P.; Floner, D.; Fourcade, F.; Amrane, A.; Geneste, F. Efficient Dechlorination of α-Halocarbonyl and α-Haloallyl Pollutants by Electroreduction on Bismuth. *Environ. Sci. Technol.* 2020, *54*, 559−567. (b) Lou, Y.-Y.; Yin, S.-H.; Yang, J.; Ji, L.-F.; Fang, J.-Y.; Zhang, S.-Q.; Feng, M.-B.; Yu, X.; Jiang, Y.-X.; Sun, S.-G. MOF-derived single site catalysts with Electron-Rich Fe-N4 sites for efficient elimination of trichloroacetamide DBP. *Chem. Eng. J.* 2022, *446*, No. 137060. (c) Dhanda, V.; Kumar, R.; Yadav, N.; Sangwan, S.; Duhan, A. Ultimate fate, transformation, and toxicological consequences of herbicide pretilachlor to biotic components and associated environment: An overview. *J. Appl. Toxicol.* 2024, *44*, 41−65.

(26) Simon, J. A.; Palke, W. E.; Ford, P. C. Photophysical and ab initio studies of mononuclear copper(I) complexes. *Inorg. Chem.* 1996, *35*, 6413−6421.

(27) For a crystal structure of (tBubpy)₂CuⅡ(OTf)₂, see: Ho, T. D.; Lee, B. J.; Buchanan, T. L.; Heikes, M. E.; Steinert, R. M.; Milem, E.

G.; Goralski, S. T.; Wang, Y. N.; Lee, S.; Lynch, V. M.; Rose, M. J.; Mitchell-Roch, K. R.; Hull, K. L. Cu-Catalyzed Three-Component Alkene Carboamination: Mechanistic Insights and Rational Design to Overcome Limitations. *J. Am. Chem. Soc.* **2024**, *146*, 25176−25189.

(28) Mukherjee, S.; Aoki, Y.; Kawamura, S.; Sodeoka, M. Ligand-Controlled Copper-Catalyzed Halo-Halodifluoromethylation of Alkenes and Alkynes Using Fluorinated Carboxylic Anhydrides. *Angew. Chem., Int. Ed.* **2024**, No. e202407150.

(29) Ritchie, C. D.; Sager, W. F. An Examination of Structure-Reactivity Relationships. In *Progress in Physical Organic Chemistry*; Cohen, S. G.; Streitwieser, A.; Taft, R. W., Eds.; Wiley, 1964.

(30) Ascorbic acid and D_2O undergoes rapid H^+/D^+ exchange at room temperature. See: Suzuki, A.; Kamei, Y.; Yamashita, M.; Seino, Y.; Yamaguchi, Y.; Yoshino, T.; Kojima, M.; Matsunaga, S. Photocatalytic Deuterium Atom Transfer Deuteration of Electron-Deficient Alkenes with High Functional Group Tolerance. *Angew. Chem., Int. Ed.* **2023**, *62*, No. e202214433.

(31) Agarwal, R. G.; Coste, S. C.; Groff, B. D.; Heuer, A. M.; Noh, H.; Parada, G. A.; Wise, C. F.; Nichols, E. M.; Warren, J. J.; Mayer, J. M. Free Energies of Proton-Coupled Electron Transfer Reagents and Their Applications. *Chem. Rev.* **2022**, *122*, 1−49.

(32) For a leading review on water as a competent H-atom donor once coordinated to a metal center, see: Boekell, N. G.; Flowers, R. A., 2nd Coordination-Induced Bond Weakening. *Chem. Rev.* **2022**, *122*, 13447−13477. However, since the Cu species in our system is coordinatively saturated by the bipyridine and Cl ligands, they are less likely to bind to water. As such, we believe that ascorbic acid (or ascorbate) is acting as the H-atom donor.

(33) March, K. *Advanced Organic Chemistry*; John Wiley & Sons, 1985.

(34) (a) Wang, H.-J.; Fu, Y.; Wang, C.; Guo, Q.-X. Theoretical Study of Homolytic C-Cl Bond Dissociation Enthalpies of Environmental Pollutants. *Acta Chim. Sin.* **2008**, *66*, 362−370. (b) Garifullina, A.; Mahboob, A.; O'Reilly, R. J. A dataset of homolytic C−Cl bond dissociation energies obtained by means of W1w theory. *Chem. Data Collect.* **2016**, *3−4*, 21−25.

(35) Weissman, M.; Benson, S. W. Heat of formation of the $CHCl_2$ radical. Bond dissociation energies in chloromethanes and chloroethanes. *J. Phys. Chem. A* **1983**, *87*, 243−244.

(36) An alternative pathway was also considered where the excited-state Cu^I ($E^{I*/0} \sim +0.95$ V vs SCE, ref 21b) undergoes reductive quenching with $AscH^-$ ($E^{•/-} \sim +0.48$ V vs SCE, ref 31). Between the two pathways, we favor the oxidative quenching mechanism described in the main text, due to its higher thermodynamic driving force.

(37) (a) Isse, A. A.; Lin, C. Y.; Coote, M. L.; Gennaro, A. Estimation of Standard Reduction Potentials of Halogen Atoms and Alkyl Halides. *J. Phys. Chem. B* **2011**, *115*, 678−684. (b) Nicewicz, D.; Roth, H.; Romero, N. Experimental and Calculated Electrochemical Potentials of Common Organic Molecules for Applications to Single-Electron Redox Chemistry. *Synlett* **2016**, *27*, 714−723.

(38) Rayne, S.; Forest, K. Gas phase homolytic bond dissociation enthalpies of common laboratory solvents: A G4 theoretical study. *Nat. Prec.* **2010**, No. 1, DOI: 10.1038/npre.2010.4425.1.